Floodplain Development, El Niño, and Cultural Consequences in a Hyperarid Andean Environment

R. B. Manners,* F. J. Magilligan,† and P. S. Goldstein‡

*Department of Geography, University of North Carolina, Chapel Hill
†Department of Geography, Dartmouth College
‡Department of Anthropology, University of California, San Diego

Using field-mapping, remote-sensing (ASTER, aerial photography), and GIS/GPS, we identified and analyzed reach-scale geomorphic responses to contemporary floods along a 20-km valley length in hyperarid southern Peru. We combined these data with alluvial stratigraphy of remnant terrace patches recording late Holocene aggradation and incision. In this manner we ascertained how climate change, especially the occurrence of the El Niño–Southern Oscillation (ENSO), affects the magnitude and frequency of large floods at mid-elevations of southern Peru's Atacama Desert, and we documented the geomorphic effects of large floods on stream channel properties, especially the large-scale floodplain erosion and channel enlargement occurring during these large ENSO-related floods. Reach-averaged channel widening of $\sim$ 30 m occurs during large ENSO-related floods, with floodplain erosion rates of 2 ha/river km commonly occurring. Recovery occurs in two stages: channel narrowing requires several decades of lateral bar development which can ultimately aggrade sufficiently for complete floodplain development to occur. There was a similar response to ENSO floods during the late Holocene, and our radiocarbon dating of alluvial surfaces, combined with an ASTER-DEM of the floodplain, indicates that $\sim$ 80 percent of the floodplain is younger than at least 550 ^{14}C years. We conclude that the lateral erosion and recovery cycle related to ENSO floods could have been a critical factor for prehistoric societies dependent on floodplain agriculture. If cultural systems can maintain pace with geomorphic change in these irrigated floodplain systems, the loss of arable land may not be critical. However, severe social stresses may result if episodes of accelerated floodplain loss outpace both natural recovery and social adaptation. *Key Words: Andes, climate change, El Niño, floods, geoarchaeology.*

In the Andean region of South America, no single climate phenomenon has had a more significant effect on past, present, and future human occupation of the region than the El Niño–Southern Oscillation (ENSO) (DeVries 1987; Grosjean et al. 1997; Fontugne et al. 1999; Kerr 1999; Sandweiss et al. 2001). Socially, regional and global-scale climatic changes have been commonly evoked to explain an array of cultural responses, including large-scale migrations and complete "social collapse" (Seltzer and Hastorf 1990; Shimada et al. 1991; Kolata and Ortloff 1996; Binford et al. 1997; Kolata 2000; Kolata et al. 2000), although critics argue that these deterministic explanations portray humans as passive players whose ability to respond to environmental change is underestimated (Erickson 1999). Both sides of this debate tend to focus on water availability per se as the critical factor in climate-related culture change. However, ENSOs are also one of the most significant vectors in the formation and modification of Andean landforms, and are particularly significant for the modification of stream channels and subsurface hydrology (Houston 2002; Houston and Hartley 2003). Other than the geomorphic signature and paleo-climatic significance of either alluvial deposits (Wells 1990; Moseley et al. 1992; Moseley and Richardson 1992; Keefer, Moseley, and deFrance 2003) or beach ridges (Richardson 1983; Sandweiss 1986; Ortlieb, Fournier, and Macharé 1993; Wells 1996; Rogers et al. 2004) in coastal Peru, there has been minimal attention paid to the broader alluvial and geomorphic effects of these events and their sociohistorical significance for riverine agricultural societies in arid regions of the Southern Hemisphere.

ENSOs, Climate Change, and Cultural Responses

There has been heightened interest recently in integrating climatic change, riparian response, and cultural adaptation, especially in characterizing channel responses to climate change (Rumsby and Macklin 1994; Wells and Noller 1999; Maas and Macklin 2002; Maas et al. 2001). Much of the geomorphic literature on channel response to large floods has focused on humid alluvial settings (Costa 1974; Pitlick 1993; Ritter et al. 1999; Magilligan et al. 1998) in Northern Hemisphere watersheds, and less is known about channel response and recovery in hyperarid streams where the thresholds

Annals of the Association of American Geographers, 97(2), 2007, pp. 229–249
Initial submission, August 2004; revised submissions, November 2005, January and March 2006; final acceptance, April 2006
Published by Blackwell Publishing, 350 Main Street, Malden, MA 02148, and 9600 Garsington Road, Oxford OX4 2DQ, U.K.

of recovery are high due to a lack of vegetation, flashy hydrologic regimes, and limited bedload mobility (Baker 1977). This contrasts with the rapid geomorphic recovery characteristic of humid regions where sustained moderate flows occur regularly, and the bed and bank material are relatively mobile. Thus, although humid environments have recovery times of $\sim 10^1$ years (Costa 1974; Magilligan and Stamp 1997), arid environments have recovery timeframes that span 10^2–10^3 years. In arid environments, Wolman and Miller's (1960) principle that the most frequent events accomplish the most work may lack validity, and large floods do most of the geomorphic work (Baker 1977). In particular, large floods spawned by ENSOs may greatly alter channels, riparian zones, and floodplains in these environments, and the geomorphic legacy of these changes may endure for $>10^2$ years (Baker 1977). The legacy of large floods is strongly climatically dependent because climate dictates channel recovery (Costa 1974; Baker 1977; Wolman and Gerson 1978; Ely and House 2000). Thus, not only are the timeframes of channel recovery amplified in arid environments, but once the system has been destabilized by a large flood, lesser magnitude events may maintain that instability and prevent geomorphic recovery from immediately occurring (Schumm and Lichty 1963).

The importance of ENSOs is critical climatically, geomorphically, and culturally in the south-central Andes. Unlike many prehistoric climate changes, which may only be detectable post facto as long-term trends, ENSOs are discrete events of relatively short duration and significant scale (Moseley 1997, 2000). As such, they may have been consciously reacted to by the societies experiencing them. Twentieth-century ENSOs and longer-term events have disrupted coastal fisheries, washed out desert settlements and irrigation systems, and caused highland famines (Chavez et al. 2003), and in the Andean region, recent research has focused on the negative effects of extreme flood and drought on settlement and agricultural systems. In this context, El Niños and related droughts are considered to be prime suspects in the retraction of human food production systems, and thus a proximate cause in the collapse of ancient societies (Moseley et al. 1983; Wells 1990; Seltzer and Hastorf 1990; Clement and Moseley 1991; Shimada et al. 1991; Satterlee 1993; Weiss et al. 1993; Kolata and Ortloff 1996; Binford et al. 1997; Moseley 1997, 2000; Williams 1997, 2002; Reycraft 2000; Satterlee et al. 2000; Weiss 2000; Caviedes 2001; deMenocal 2001). Although the destructive power of ENSOs cannot be disputed, "catastrophic" scenarios have been questioned, both on empirical grounds (cf. Chapdelaine 2000) and theoretically, as "neo-environmental determinism" (Erickson 1999, 2000). Moreover, El Niños may have had profound positive impacts (Sandweiss et al. 1998, 2001) and be associated with monument building and the emergence of complex societies after the initial mid-Holocene onset of ENSOs.

In hyperarid riverine agricultural regimes, consideration of the cultural effects of ENSO and related phenomena has been couched in terms of the availability of water itself—by focusing on the cultural effects of prolonged droughts (Seltzer and Hastorf 1990; Shimada et al. 1991; Kolata and Ortloff 1996; Binford et al. 1997); the destructive effects of flood events on water delivery systems (Clement and Moseley 1991; Huckleberry 1999; Williams 2002; Huckleberry and Billman 2003); and the devastating effects on villages and populations of debris flows spawned by ENSOs (Satterlee 1993; Keefer, Moseley, and deFrance 2003). It is therefore not surprising that most of these studies highlight catastrophic rather than interactive or adaptive interpretations of the human–climate interaction. We propose that the cycle of flood-related loss and subsequent recovery of agricultural floodplain lands is an important and overlooked variable in studies of the cultural adaptation to riverine agriculture in hyperarid regions. Valley-bottom lands (floodplains and terraces) have both a significant hydraulic/energetic advantage in their proximity to the river, and a fertility advantage because of the floodplain's active sedimentation and soil development. Although both ancient and modern farmers utilized both valley-bottom floodplain and valley-side reclaimed lands, the valley-bottom floodplain lands are considerably more productive and today command prices of more than $20,000/ha. Because of the deeply incised topography of the south Andean valleys, the irrigable valley-bottom floodplain land is both extremely limited in extent and highly susceptible to disturbance by floods. To evaluate how these societies have adapted to working these high-risk, high-benefit lands, it is fundamentally important to first understand the cycle of loss and regeneration of this limited agricultural resource.

Our research investigates the magnitude and rates of landscape and environmental change in a hyperarid section of southern Peru by documenting the geomorphic effects of large floods on stream channel properties, especially the large-scale floodplain erosion and channel enlargement occurring during large ENSO-related floods. First, through detailed field-mapping and the utilization of remote-sensing (aerial photographs, ASTER) and GIS/GPS, we characterized the geomorphic effects of contemporary large floods in the Moquegua Valley of southern Peru's Atacama Desert and

determined the magnitude and rate of geomorphic effects in hyperarid regions where the legacy of effects may persist for decadal, or longer, timescales (cf. Baker 1977). Second, we used established regional and local alluvial chronologies to develop a late-Holocene record of channel changes to large floods. Third, we documented the interrelatedness between the type, direction, and tempo of channel and riparian adjustments to ENSO-related large floods and the sociocultural realm by characterizing the rates by which in-channel post-flood depositional features are converted to arable land. In this way, we are able to link the timescales of geomorphic recovery to the broader cultural arena.

Study Area

This current study focuses on the mid-valley Moquegua Valley in southern Peru (Figure 1). Because of its regional setting, the Rio Moquegua is strategically situated to record the occurrence of ENSO-related floods, as Southern Oscillation–derived events dictate flood magnitude and frequency. The Rio Moquegua heads in the south-central Andes and flows westward into the Pacific Ocean near Ilo, Peru. The valley is situated in the northern fringes of the Atacama Desert and annual precipitation rates are limited ($\sim$ 75–100 mm/yr) but increase with altitude (Satterlee et al. 2000; Houston and Hartley 2003). For this part of southern Peru, two flood-producing mechanisms exist: localized ENSO-related precipitation and rain/rain-on-snow in the highland Andes during La Niñas. Climatically, wet and dry periods in the Bolivian Altiplano correspond to high and low index phases of the Southern Oscillation, respectively (Vuille 1999). The dominant surface atmospheric circulation over the Bolivian Altiplano, known as the Bolivian High, is formed during summertime heating that coincides with an increase in moisture-bearing trade winds. The strength and position of the Bolivian High modulates rainfall anomalies. During low-index phases (El Niño) of the Southern Oscillation, the Bolivian High decreases in strength and shifts southward, weakening easterly winds and further reducing movement of moisture onto the Altiplano. The opposite occurs during high-index phases (La Niña), pushing the High northward and allowing for wetter summers (Vuille 1999; Baker et al. 2001; Placzek, Quade, and Betancourt 2001). Therefore, La Niñas potentially indicate large rainfall events over the Altiplano, prompting Andean runoff into the Moquegua Valley and causing large floods. This effect indeed occurred in March of 1997

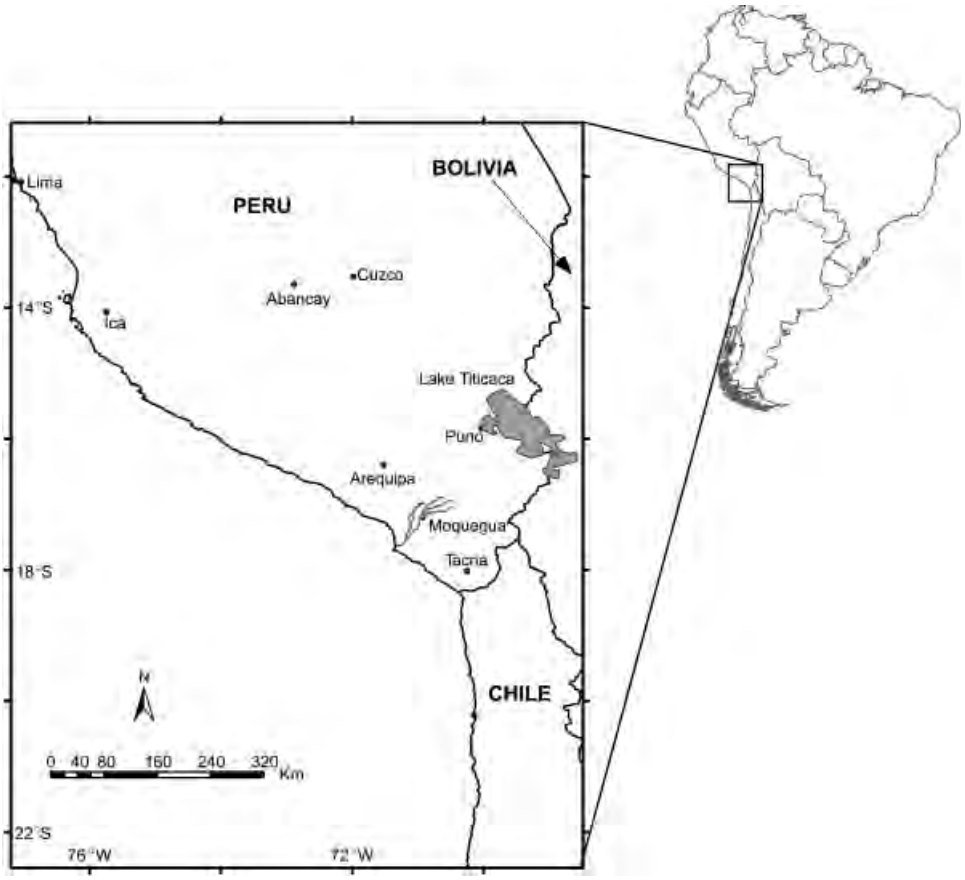

Figure 1. Map of south-central Andes with enlargement of Moquegua River Valley.

when an extremely large flood hit the mid-valley of the Rio Moquegua despite the lack of rain occurring on mid-elevation western slopes. Residents spoke of an extreme short duration event that lacked corresponding rainfall in the mid-valley section of the basin. According to local officials and residents, the March 1997 flood was of a greater magnitude than the immediately subsequent El Niño flood in March of 1998 where sustained localized precipitation occurred (Magilligan and Goldstein 2001).

Our study focuses on the ~ 20-km mid-valley of the Rio Moquegua which heads near the town of Moquegua, Peru, and ranges in elevation from ~ 1350 m to ~ 980 m. The regional geology consists of a series of Tertiary sedimentary and volcanoclastic rocks that are capped in places by Quaternary alluvial gravels (Tosdal, Clark, and Farrar 1984; Gregory-Wodzicki 2000). More resistant igneous rocks crop out irregularly along the mid-valley, and the distal section of the mid-valley terminates where the channel flows into these resistant lithologies. The area is tectonically active and earthquakes are common hazards. A 7.9 quake (Richter scale), centered near Arequipa, Peru, occurred in 2001, causing widespread structural damage in Moquegua more than 200 km away. This was also the approximate site of a massive quake and eruption that occurred in AD 1600 (Thouret, Davila, and Eisen 1999), spewing ash into the Moquegua Valley. This ash is readily identifiable in hillslope deposits and alluvium and is an important stratigraphic marker in the basin fill (Magilligan and Goldstein 2001).

Modern land use in the Moquegua Valley is primarily irrigated floodplain agriculture (Figure 2), with some amplification of irrigation to reclaim more distant desert lands. Canal systems for water delivery range from state-operated cement-lined canals to hand-dug ditch systems. The earliest dates of floodplain farming may precede the beginning of an indigenous ceramic tradition in the Moquegua Valley, known as Huaracane (385 cal BC–cal AD 340). Huaracane settlement and subsistence patterns suggest a nonspecialized agrarian subsistence strategy. Represented by 169 habitation components, the Huaracane domestic occupation in the Moquegua Valley totaled 73.5 ha in residential area, with all but five domestic components under 2 ha in size, suggesting a generally low level of political and economic centralization (Goldstein 1989, 2000b, 2005). Huaracane habitations were found on virtually every hilltop or slope

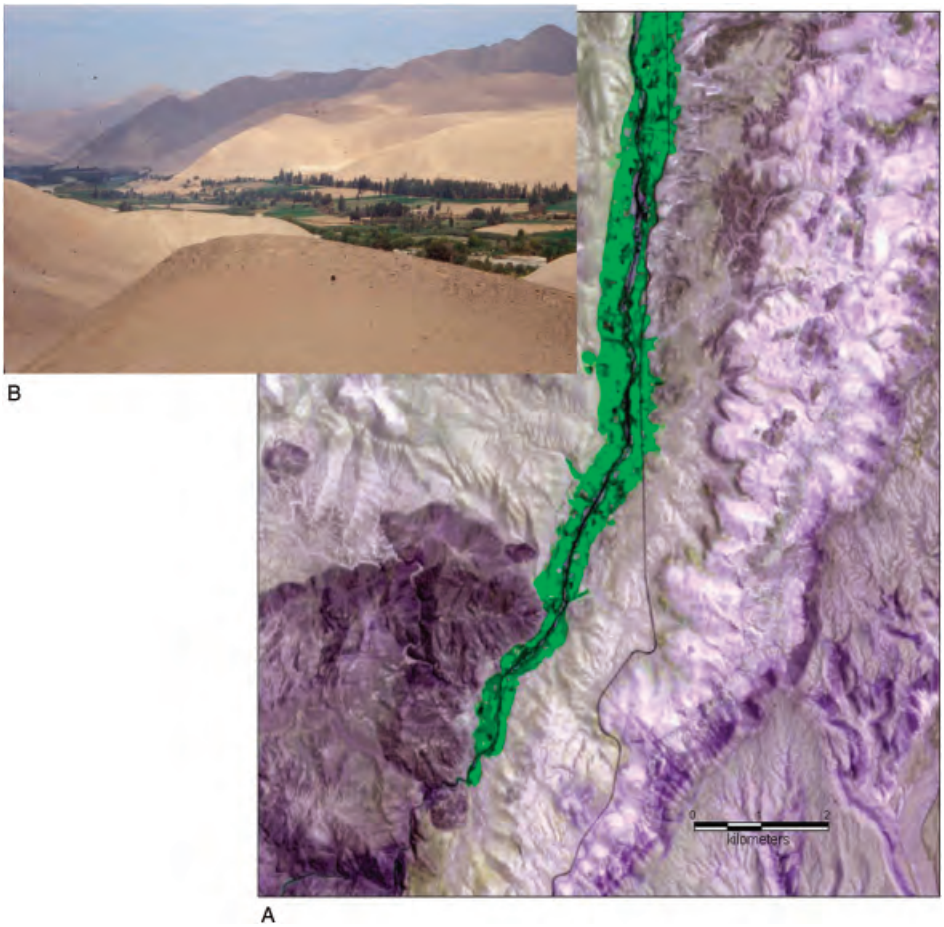

Figure 2. Photos of Moquegua Valley. Top photo (A) is downvalley view showing the well-vegetated irrigated floodplain irrigation and the completely dry and vegetation-free valley-sides. Bottom image (B) is 2000 ASTER image of the lower 10 km of valley. Vegetation is shown in green.

along the rim of the valley-bottom in the study area, at an average elevation only 48 m above the river level. This close relation to the floodplain indicates a reliance on simple valley-bottom canals. This distinguishes Huaracane's agrarian strategy from those of subsequent, politically more complex societies, notably the Tiwanaku colonization of the region (AD 600–1000). Tiwanaku's far larger settlement enclaves were located far from the valley and were associated with the reclamation of desert pampas through extensive canals or supplementary groundwater sources for surplus maize production (Williams 2002; Goldstein 1993, 2000a, 2003, 2005). Following the Tiwanaku collapse, most of these extended irrigation systems were abandoned in the middle valley, and through the Inca, Spanish Colonial, and historic periods, agriculture again focused on the highly fertile valley-bottom lands.

Data Sources, Field Methods, and Statistical Analyses

This study relied on several approaches to document the spatial and temporal response to ENSOs. For reach scale changes, we utilized a combination of remotely-sensed data (airphotos and ASTER) and combined these with contemporary GPS field mapping of riparian geomorphology. This reach-scale analysis was augmented with a finer scale spatial resolution to better identify which floodplain sections respond to and recover from ENSO-related floods. Holocene floodplain adjustments were ascertained by detailed alluvial stratigraphy and radiocarbon dating of buried paleosols to compare twentieth-century fluvial adjustments to millennial scale adjustments.

Remote Sensing

Aerial photographs of the Moquegua Valley were obtained and scanned at high resolution (4200 dpi) and subsequently georectified to a set of 1997 cadastral maps in ArcMap using the Universal Transverse Mercator projection with the Provisional South American Datum for Venezuela 1956. The five sets of photographs (1946, 1955, 1970, 1976, and 1997) span fifty-one years and were used to document the sequence and style of channel adjustments to large floods in an approach similar in design to the recent work by Winterbottom (2000), Poole et al. (2002), Rinaldi (2003), and Rogers et al. (2004). Although temporally rich (51 years), not all of the basin is covered completely over this timespan. Because of selective differences in basin coverage from successive photographs, we developed a temporally intensive analysis where the upper 9.9 km of the basin has robust sequential coverage (51 years). The temporally intensive coverage was augmented by a spatially intensive analysis wherein the entire basin (total river length of 19.5 km) is covered, but has only 33 years of coverage.

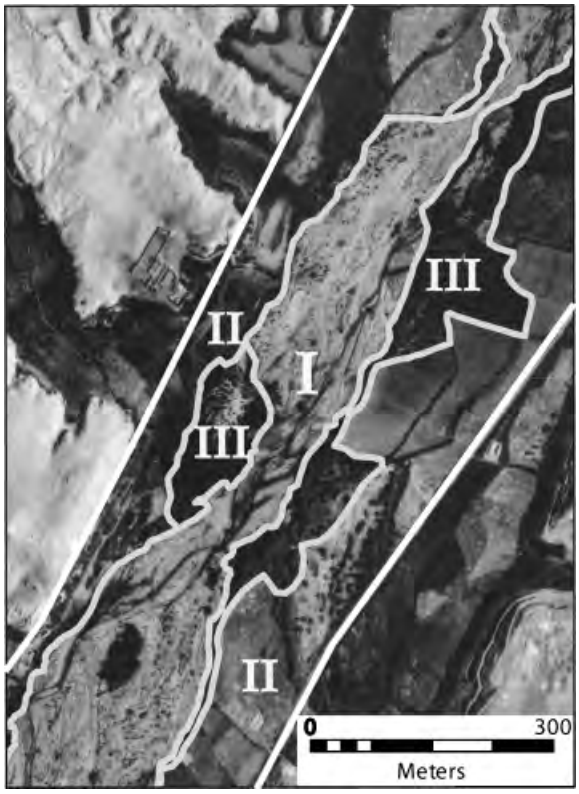

Figure 3. Aerial photograph showing methods employed for GIS mapping. For each photo we drew vectors delineating active channel (I), arable land (II), and floodplain under construction (III) and calculated surface areas for each land use category for each image and photo set.

Using ArcMap, vectors were delineated on each photo set for (a) arable land, (b) the active channel, and (c) land deemed "floodplain under construction" (Figure 3). This was done for the entire 19.5 km stretch of the Rio Moquegua from its confluence with the Tumilaca and Torata Rivers, downstream to where the valley narrows then enters a highly constrained bedrock gorge. The active channel was determined to be the gravel-dominated areas possibly containing some shrub but with no dense vegetation (Sloan, Miller, and Lancaster 2001). Plowed land with crops as well as land absent of crops but in a state that appeared to be able to support crops was labeled arable land. Dense vegetation within the riparian zone adjacent to channel margins was classified as "floodplain under construction" (Figure 3). In essence, this category characterizes the deposition and

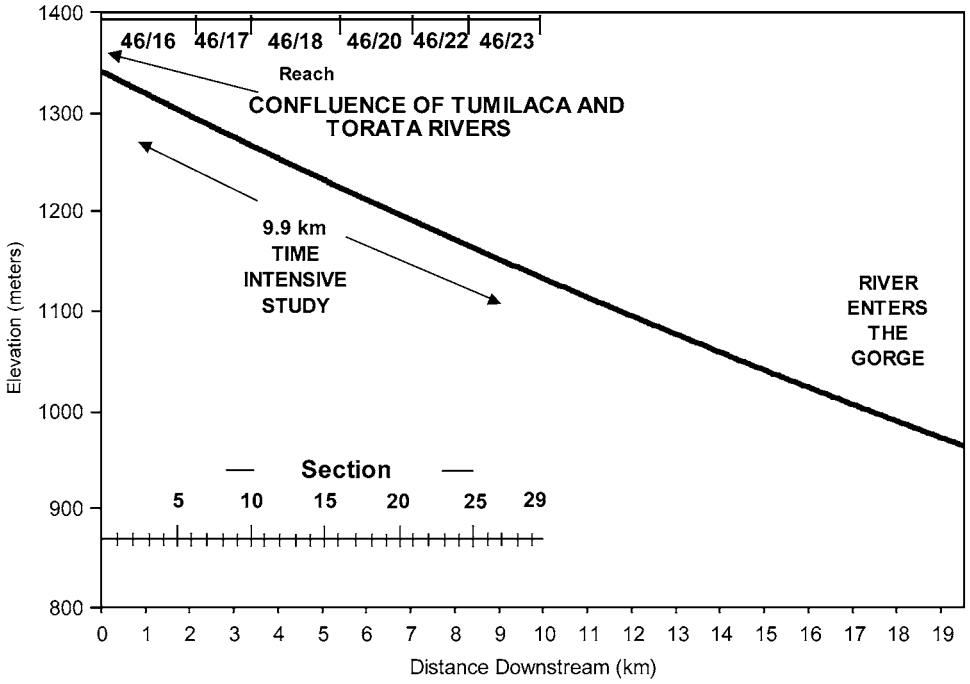

Figure 4. Longitudinal profile of the 19.5 km mainstem of the mid-valley Rio Moquegua based on 2003 ASTER DEM. Along the upper diagram are the portions of the valley divided into reaches that are the basis for the composite interpretation for the image analysis (in order: Reaches 46/15, 46/17, 46/18, 46/20, 46/22, and 46/23). At the bottom of the image are the locations of the sections (Sections 1–29) for the upper 9.9 km of the basin.

colonization of side-channel lateral bars by shrubs and trees. Because no aerial photographs exist post-1997, contemporary geomorphic and riparian conditions were field-mapped in 2003 by a field team using GPS and walking both sides of the 19.5 km channel/riparian zone. We created vectors consistent with those mapped from the aerial photographs based on the same field criteria. GPS field data were differentially corrected to local base stations nightly.

To quantify the continual reworking and lateral migration of the river, we use transition probability matrices (equation (1)) to characterize the shift from one riparian condition (active channel, arable land, floodplain under construction) to another between successive photo sets:

$$p_{ij} = \text{Prob}[X_{t+1} = j | X_t = i]. \quad (1)$$

Many studies use this statistical tool as a means to assign the probability of some condition (j) being in a discrete state at time $t+1$, given that it was in another discrete state (i) at time t (Formacion and Saila 1994; Selim and Al-Rabeh 1995; Yu and Yang 1997). In this study, we used this tool as a means of characterizing the actual transitions. Therefore these matrices do not actually represent a probabilistic model but instead capture and represent the percentage of land use change from one period to the next.

Reach Scale Geomorphic Response

The channel bed longitudinal profile is relatively constant ($\sim$ 1.8 percent slope), lacking any significant gradient changes or knickpoints (Figure 4). To track and systematically compare changes between photo sets, we segmented the photos into reaches of $\sim$ 1–2 km, and then further into finer scale sections of $\sim$ 350 m. In this way, we could identify the changes in channel position and morphology across two scales. Because channel response and recovery to large floods are conditioned by channel position within the valley and by differences between valley and channel strike (Miller 1995), we developed a dimensionless index that characterizes the channel position relative to valley controls (equation (2)). Valley width, valley midpoint, channel midpoint, and channel width were measured in ArcMap at a cross section marking the beginning of each reach and at 350 m intervals through each section. To document temporal changes, each of the reaches was measured for each of the six time periods represented (1946–2003). Those data were subsequently entered into equation (2) to determine the Index of Channel Movement (I_{cm}). This index isolates reaches that are geomorphically active throughout the study period, tracks the channel's movement within the valley, and indicates its location over time from the valley wall to the middle of the valley. As the channel approaches the valley side (away from the valley midpoint), I_{cm} approaches 0.5. I_{cm} values close to 0 correspond to the channel being near the middle of the valley:

$$I_{cm} = \frac{[\text{Valley midpoint} - \text{Channel midpoint}]\,\text{m}}{[\text{Valley width}]\,\text{m}}. \quad (2)$$

Climatic Metrics

We used published records of ENSOs to provide the climatic context (Quinn, Neal, and Antunez de Mayolo 1987; Ortlieb and Machare 1993; Ortlieb 2000). Using historical and maritime archives, Quinn, Neal, and Antunez de Mayolo (1987) compiled a 450-year regional history of El Niño magnitude and frequency, and ranked the relative intensity of ENSOs. La Niña occurrences were derived from Pacific Ocean pressure differences, otherwise known as the Southern Oscillation Index (SOI), with high-index phases (positive SOI) corresponding to La Niñas. Because floods more commonly occur in the austral fall, we determined the SOI values solely for February and March to more accurately portray the regional hydroclimatology. For our study area, large floods result from SOI extremes, although the moisture sources differ radically.

Holocene Alluvial Chronologies

While mapping the river margins in August 2003, we also collected datable material in floodplain alluvium where it was exposed along the Rio Moquegua. Samples were collected to augment established alluvial chronologies and floodplain dates (Magilligan and Goldstein 2001) and were dated by traditional radiocarbon methods. Using various floodplain terraces found along the study stretch, we documented the longitudinal and cross-valley pattern of Holocene lateral reworking of the valley. We correlated floodplain terrace dates with terrace heights above the channel bed to establish an age-height relationship for the alluvial fill. Although sampled as close to the terrace base as possible, some of the dates do not completely represent basal dates and are considered minimum ages for the terraces. Terrace heights above the channel bed were measured with a TOPCON total station. A 2003 ASTER image was converted to a 30-m ASTER-based digital elevation model (DEM). From the DEM, 2 m contours were overlaid in ENVI® and exported as a shapefile to ArcMap. The floodplain topography was mapped and ultimately contoured as heights above the channel bed (in 2-m contours); the downstream suite of bed elevations was determined by the bed elevations along the longitudinal profile (see Figure 4). In this way, we were able to approximate the age of alluvial surfaces throughout the valley based on elevations and ultimately determine the percentages of the total valley at various estimated ages.

Results

In general, our results indicate the fundamentally dynamic nature of alluvial responses in the Rio Moquegua with differential lag times of alluvial and agricultural recovery occurring. The 10 km portion of the Rio Moquegua available for the time-intensive analysis (1947–2003), Reaches 46/15 to 46/23 (Figure 4), shows that considerable channel widening (and consequently floodplain loss) occurred between 1946 and 1955 (Figure 5). Within this nine-year period, mean channel width increased by $\sim$ 30 percent, resulting in a loss of about 19 ha of land ($\sim$ 2 ha of erosion/river km), 14 ha of which had been cultivated. Conversely, the 1955–1970 and 1976–1997 periods showed gradual, yet substantial, channel and floodplain recovery. The cumulative change over the two recovery periods corresponds to a mean channel narrowing of $\sim$ 30 m. Channel recovery during this forty-two-year period (1955–1997) is even more evident in the composite transition probability matrix (Table 1). For both periods (1955–1970 and 1976–1997), the probability that the active channel remained an active channel was 68 percent (Table 1b) and 65 percent (Table 1d), respectively, suggesting that what had initially been active channel has either been converted to arable land or to floodplain under construction. These figures differ from the initial widening phase of 1946–1955, when the amount of active channel remaining as active channel was 92 percent (Table 1a). The striking difference between these two stable periods is the disparity between the rates of change of arable land. While the channel recovers from whatever destabilizing event (or events) occurred between 1946 and 1955, the percentage of arable land stayed fairly constant up to 1970 (Figure 5). This differs from the sharp

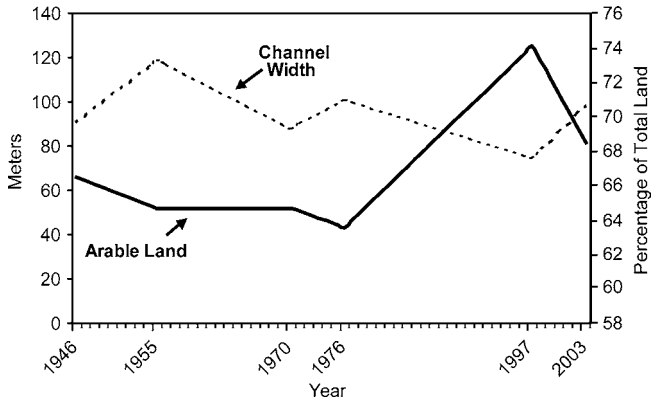

Figure 5. Time series of mean channel width and percentage of arable land for the fifty-seven-year study period. These data are the composite 9.9 km reach-averaged values for the upper study area.

Table 1. Transition probability matrices for conversion of one land cover (active channel, floodplain under construction, or arable land) to another land cover for successive photos

Photo dates		Active channel	Floodplain under construction	Arable floodplain
(a) 1946–1955			**1946**	
1955	Active channel	0.92	0.36	0.05
	Floodplain under construction	0.07	0.36	0.02
	Arable floodplain	0.01	0.28	0.93
(b) 1955–1970			**1955**	
1970	Active channel	0.68	0.34	0.01
	Floodplain under construction	0.23	0.4	0.04
	Arable floodplain	0.1	0.25	0.96
(c) 1970–1976			**1970**	
1976	Active channel	0.85	0.24	0.04
	Floodplain under construction	0.12	0.57	0.03
	Arable floodplain	0.03	0.19	0.93
(d) 1976–1997			**1976**	
1997	Active channel	0.65	0.18	0.01
	Floodplain under construction	0.15	0.31	0.01
	Arable floodplain	0.2	0.51	0.98
(e) 1997–2003			**1997**	
2003	Active channel	0.92	0.45	0.05
	Floodplain under construction	0.07	0.46	0.04
	Arable floodplain	0.01	0.09	0.91
(f) Composite: 1946–2003			**1946**	
2003	Active channel	0.8	0.44	0.04
	Floodplain under construction	0.11	0.27	0.03
	Arable floodplain	0.09	0.29	0.92

Note: This represents the probability transition matrices for the upper 9.9 km of the valley where the more robust temporal coverage occurs.

increase in arable floodplain (a gain of 44 ha) that occurred between 1976 and 1997 (Table 1 and Figure 5).

This increased area of arable floodplain is further revealed by the transition probability matrix from 1976 to 1997 (Table 1d), which shows the probability of both active channel and floodplain under construction becoming arable land as 0.20 and 0.51 respectively. The areal increase revealed for conversion to arable land exceeds that of any other sequential photo set. The active channel to arable land transition ranges from as low as 0.01 to 0.10 among the other matrices (Table 1), with a combined probability (1946–2003) at 0.09 (Table 1f). The floodplain under construction to arable land rate ranges from 0.09 to 0.28, with a combined probability (1946–2003) of 0.29. Additionally, the probability of a square meter of land that was arable in 1976 remaining arable in 1997 is 0.98 (Table 1d), again much higher than any of the other time slices (with the probabilities falling between 0.91 and 0.96), suggesting that channel activity was especially limited between 1976 and 1997.

Channel width should correlate with changes in the amount of arable land as changes in width would seem to dictate a gain or loss of this landcover type. Indeed, such a relationship has been loosely established (Figure 5), indicating that from 1946 to 1955 as the channel widened, the amount of arable land decreased. Yet the relationship does not hold as strongly during channel-narrowing phases (1955–1970 and 1976–1997) as the riparian system begins to recover. The transition is not physically sequential because floodplain development to arable land requires the intermediate stage of lateral bar development, which then requires sufficient time to convert to arable land. The amount of arable land in the period 1955–1970 stayed relatively stable (Figure 6), but despite the overall constant area in arable land during this period, considerable channel narrowing occurred. The disparity results from areal changes in land classified as floodplain under construction: that increase explains the noted landcover changes, with a 75 percent increase in this fifteen-year timespan. In terms of probabilities, there is a 0.23 probability that the active channel in 1955 would become floodplain under construction by 1970 (Table 1b). In 1976 the percentage of arable land begins to increase, and the amount of floodplain under construction declines.

Separating out these landcover types reveals that recovery occurred in two distinct steps. After considerable

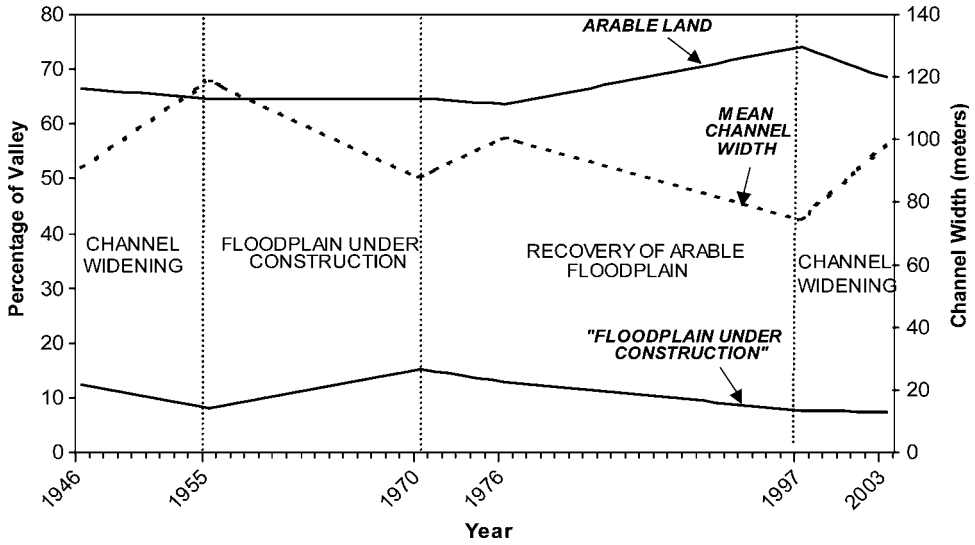

Figure 6. Time series of mean channel width, floodplain under construction, and percentage of arable land for the reach-averaged upper 9.9 km section of the upper mid-valley. Also shown is the dominant channel/floodplain activity occurring in discrete time periods. Note how channel narrowing is first accomplished by increased area of floodplain under construction (1955–1970) and how arable land increases after 1970 even while the channel widens from 1970–1976. The increased channel widening occurs through erosion of lateral bars, not arable floodplain. The sequence of floods in 1997 (La Niña) and 1998 (El Niño) greatly increases channel width, primarily through erosion of arable floodplain land.

lateral reworking between 1946 and 1955, a lag time exists in the recovery of arable land, coinciding with a substantial increase in the amount of floodplain under construction. The recovery culminates in 1997, attaining conditions similar to those that existed in 1946. After 1997, the Moquegua Valley experienced two sequential extreme events (La Niña in 1997 and El Niño in 1998), causing similar valley reworking with major channel expansion. However, this period of channel widening differed from that of the 1970–1976 period (Figure 6) in that the channel widening from 1997–2003 resulted in a loss of arable land, not the lateral stripping of floodplain under construction that occurred in 1970–1976 (Figure 6). At the composite scale for the upper 9.9 km, the meander-belt (active channel plus floodplain under construction) ranged from 36 percent of the valley in 1976 to 26 percent in 1997 when the channel was at its narrowest. This indicates that on contemporary, decadal timescales, 76 percent of the valley was immune to lateral channel reworking; most of the lateral reworking occurred in 24–36 percent of the riparian land.

For the most downstream sector of the survey, coverage was limited to only two photo sets (1970 and 1997) and our 2003 GPS field surveys. Most of the

Table 2. Transition probability matrices for conversion of one land cover (active channel, floodplain under construction, or arable land) to another land cover for successive photos

Photo date		Active channel	Floodplain under construction	Arable floodplain
(a) 1970–1997			**1970**	
1997	Active channel	0.72	0.22	0.02
	Floodplain under construction	0.16	0.48	0.02
	Arable floodplain	0.12	0.3	0.96
(b) 1997–2003			**1997**	
2003	Active channel	0.85	0.28	0.03
	Floodplain under construction	0.09	0.57	0.03
	Arable floodplain	0.05	0.15	0.94
(c) Composite: 1970–2003			**1970**	
2003	Active channel	0.71	0.36	0.03
	Floodplain under construction	0.16	0.44	0.04
	Arable floodplain	0.13	0.23	0.94

Note: This represents the probability transition matrices for the lower (9.9–19.5 km) portion of the valley where a less robust temporal coverage occurs.

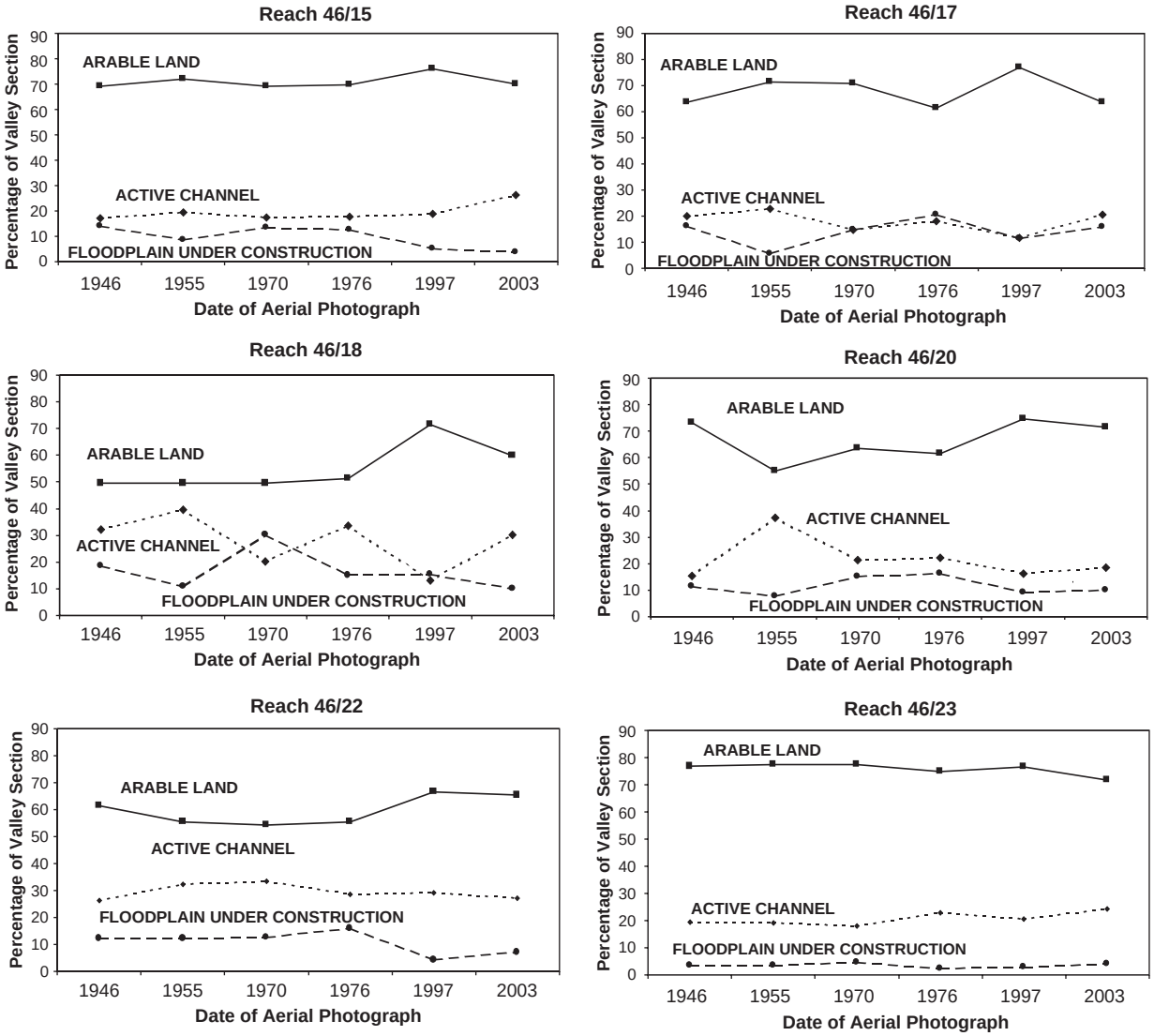

Figure 7. Reach by reach change in arable land, active channel and floodplain under construction over time. For location of reaches, see the longitudinal profile in Figure 4.

period of time covered by the aerial photos corresponds to significant channel recovery for the upper 9.9 km (Figures 5 and 6). The transition probability matrices for the lower half of the mid-valley show similar recovery trends (see Table 2). Between 1970 and 1997, there was a major transition of active channel to either floodplain under construction (0.16) or to arable land (0.12) (Table 2), with a probability of 0.30 that the floodplain under construction would be transformed to arable floodplain (Table 2). This trend of increasing arable floodplain up to 1997 mirrors in many ways the transitions for the upper 9.9 km of the valley, although there is no 1976 photo for the downstream section to make the comparisons more complete. The sequence of floods in 1997 and 1998 affected the downstream reaches less dramatically. The probability that an active channel in 1997 remained an active channel in 2003 is 0.85 for the lower reaches (Table 2) and 0.92 for the upper section (Table 1e). During these floods in 1997 and 1998 there was a ~ 9 percent loss of arable land in the upper reaches (Table 1e) and 6 percent loss in the lower reaches. The transition of floodplain under construction to arable land was 0.15 between 1997 and 2003; the same period saw a transition of only 0.09 for the upper reach (Table 1e).

Reach Scale Channel-Floodplain Adjustments

The previous analysis focused on the aggregate change of the mid-valley, especially for the more tem-

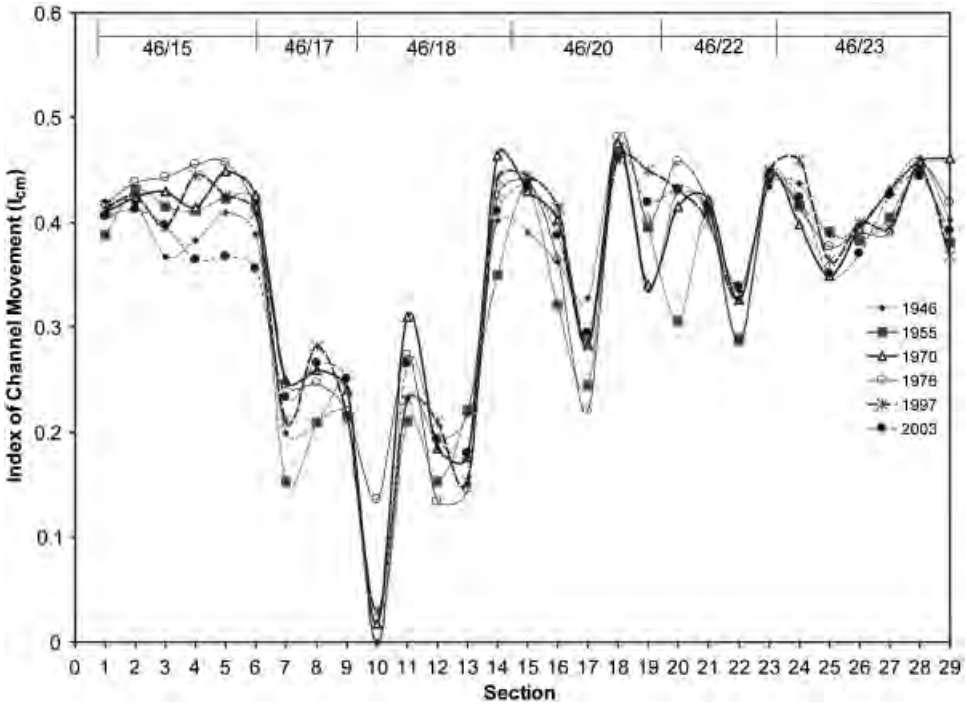

Figure 8. Index of channel movement (I_{cm}) over time for each section. The index is based on equation (2) and represents channel movement for the upper 9.9 km of the valley. Reaches are delineated at top axis and sections are located on bottom axis.

porally complete upper 9.9 km. A more spatially focused analysis begins to highlight which reaches and sections are most responsive. Minimal geomorphic change occurred in the most upstream reach, Reach 46/15, and in the two most downstream reaches, Reaches 46/22 and 46/23 (Figure 7). The composite upper mid-valley generally experienced channel widening and lost arable land between 1946 and 1955 (Figure 5), however Reach 46/15 shows minimal change during this same time period. It is primarily a fairly stable reach throughout most of the period of analysis (1946–2003) although it did lose arable land following the floods in 1997 and 1998 (Figure 7). The lower two reaches also changed minimally, especially the most downstream reach (Reach 46/23), which was the least sensitive composite reach. The lack of change in this reach is attributable to its wide and straight channel and its relatively fixed location where it hugs the right valley-side throughout the period of record (Figure 8).

Most of the alluvial reworking occurred in the next three downstream reaches (Reaches 46/17, 46/18, and 46/20). This enhanced activity was manifested primarily in Reach 46/20 (Figure 7) where the amount of arable land fell to a minimum value of 56 percent of the valley in 1955 (Figure 9 and Figure 7). Following this channel-widening episode, progressive change occurred in the accumulation of arable land, which increased to 75 percent of the valley in Reach 46/20, corresponding to its initial maximum value in 1946 (thirty-one years to recover). After major floodplain erosion between 1946 and 1955, Reach 46/20 became relatively more stable. The channel generally straightened out after 1955 and flowed more parallel to valley strike, ultimately diminishing major lateral reworking. If, as is the case in Reach 46/20, flow is transverse to valley axis, then floodplain destruction more commonly occurs (Miller 1995). But as the river adjusts and recovers from the initial disturbance, it becomes less transverse and major geomorphic activity attenuates. At a finer scale of analysis, three of the five sections in Reach 46/20 were the three most active sections in the entire study site. Section 17 shows some of the most reworking of all the sections, with the 1955 channel not occupying any of the 1946 channel (Figure 9). This section possesses the most drastic difference in valley and channel orientation, with an 18-deg difference in valley and channel strike.

To explain geomorphic controls on long-term changes at the section scale, we determined the cumulative sum of the absolute value of channel narrowing and widening (I_{cm}) and used it as an expression of total geomorphic activity because some sections never widened or narrowed whereas other sections "accordioned" in width over time. The cumulative channel change by width is plotted against I_{cm} (equation (2)) to determine if channel position in the valley (and its variation over time) explains the cumulative change in channel width (Figure 10). For many sections, the stable channel

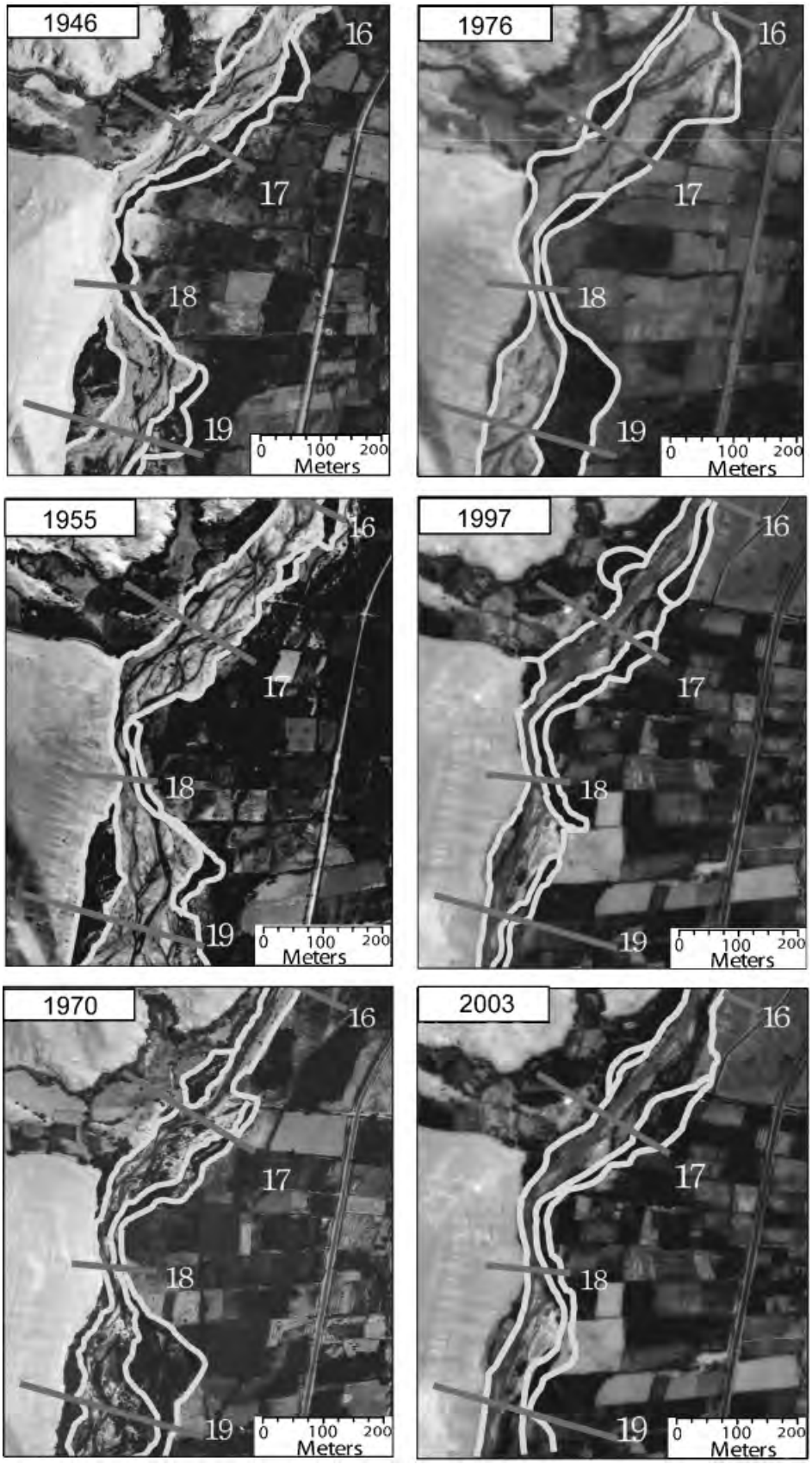

Figure 9. Time series of aerial photos with mapped vectors for Reach 46/20 for 1946, 1955, 1970, 1997, and 2003. Sections are located on each photo. For location of sections, see the longitudinal profile in Figure 4.

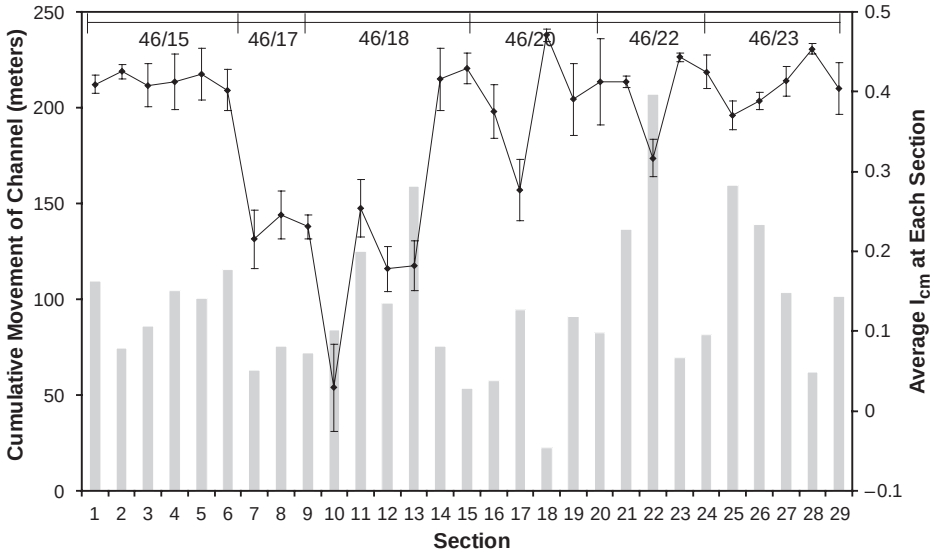

Figure 10. Mean value of the Index of Channel Movement (I_{cm}) at each section and the cumulative movement of the channel at each section. For the mean I_{cm} at each section, the standard deviation is shown by vertical bars. For the cumulative movement of the channel, it represents the sum of the absolute value of channel width (narrowing or widening) over the fifty-seven-year time period; the Index of Channel Movement indicates the position of the channel relative to the valley side or the middle of the valley.

position over time along the right valley side ($I_{cm} \rightarrow 0.5$) and its minimal variance over time help to explain the lack of sustained geomorphic activity (Figure 11). Sections showing the greatest cumulative channel activity (cumulative widening and narrowing) seem to correspond to high variance in I_{cm} (error bars in Figure 10) almost irrespective of mean channel position. Sections and reaches showing the greatest cumulative change correspond to a highly variable I_{cm} or to where the channel shifted its mean position from the valley wall to the mid-valley or vice versa (Figure 10).

ENSO Controls on Geomorphic Change

Using mean channel width as a proxy of geomorphic stability, we relate channel change to climatic controls and flooding events. Separating possible flooding events into two possible categories, El Niño–induced and La Niña–induced, permits distinction between the geomorphic effects of these events. The temporal changes in SOI, ENSO frequency and magnitude (Quinn, Neal, and Antunez de Mayolo 1987; Wolter and Timlin 1998; McPhaden 1999), and mean channel width are compared (Figure 12). Matching specific ENSOs with channel change is often inexact for several reasons. The SOI measures oceanic pressure differences that may not materialize directly in terrestrial precipitation. Similarly, because of the spatial variation in precipitation magnitude and intensity, it is possible that ENSO events delimited by SOI may not have as large an impact in the Moquegua Valley. This may explain why the 1982–1983 ENSO failed to manifest geomorphologically in channel change in the mid-valley reaches of the Rio Moquegua, even though it was of similar ranking to the 1997–1998 ENSO, which caused major floodplain erosion (cf. Figures 6 and 12). The 1982–1983 event may have been a profound ENSO as measured by SOI, but synoptic controls may have limited it moving inland from the coast where major flooding occurred (Wells 1990).

The temporal pattern of the SOI and La Niña episodes seems to correspond well with fluvial activity in the Rio Moquegua. The lack of climate stations or stream gages precludes exact correlation, but a geomorphic signal seems to appear (Figure 12). Wolter and Timlin (1998) suggest decreased frequencies of La Niñas between 1976–1997 and Chavez et al. (2003) posit an increased sea surface warm phase from 1975 to the mid-1990s. The lack of La Niñas may help explain the minimal channel erosion in the Moquegua Valley during the same period.

Linking the climatic signal to fluvial response may not be a simple one-to-one correspondence, nor can we specifically separate out the relative importance of La Niña from El Niño events (except in the later record where regional information is more available). During the past fifty-seven years of aerial photographs, major geomorphic work was done between 1946 and 1955, with significant channel widening occurring. In that time, two ENSO events are noted (Figure 12), one that was weak-to-moderate and the other moderate-plus (Quinn, Neal, and Antunez de Mayolo 1987). Neither of these events seems to have been on the order of magnitude to generate major valley reworking, however 1950 was a particularly strong La Niña year, with an average SOI in February and March of 17.6 (Figure 12). The geomorphic changes noted in Figure 12 may result from this one event, or major floodplain erosion could have resulted from the cumulative effects of the two

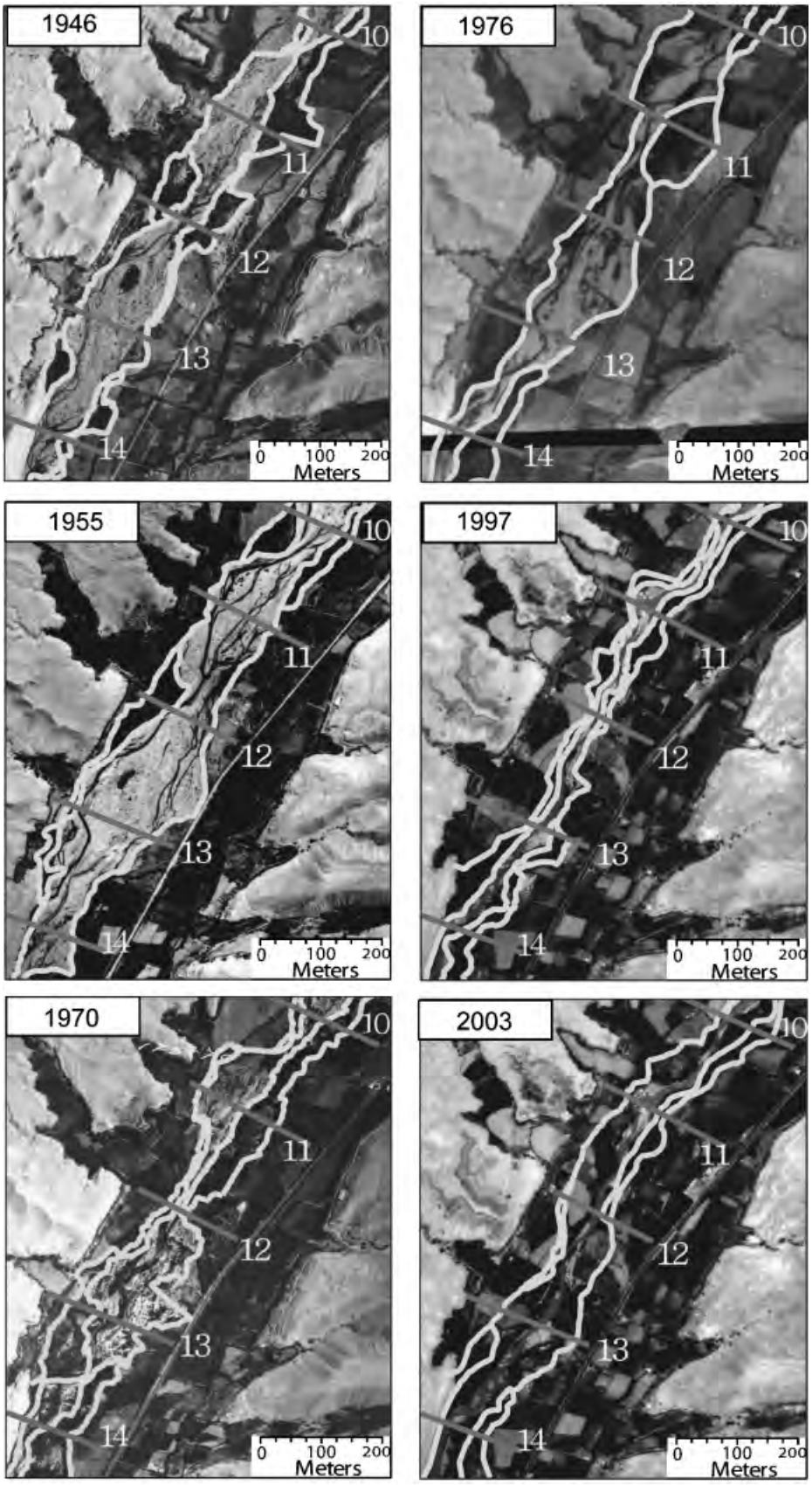

Figure 11. Time series of aerial photos with mapped vectors for Reach 46/18 for 1946, 1955, 1970, 1997, and 2003. Sections are located on each photo. For location of sections, see the longitudinal profile in Figure 4.

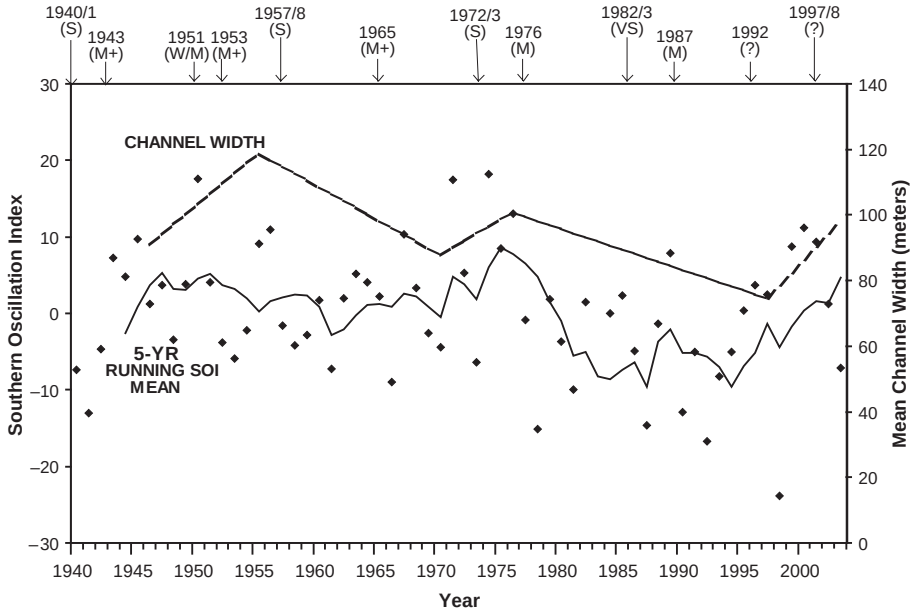

Figure 12. Time series of calculated mean channel width and the occurrences, intensities, and measures of the El Niño–Southern Oscillation (ENSO). Along the upper portion of the diagram, we use the occurrences and intensities from Quinn, Neal, and Antunez de Mayolo (1987) where W = weak, M = moderate, S = strong, and VS = very strong. For the 1997/8 El Niño, we use Wolter and Timlin (1998). The SOI time series is based on the February–March Pacific Ocean sea surface pressure differences, and the SOI graph is the five-value moving average.

ENSO events, or even a combination of all SOI-related events.

Late Holocene Alluvial Adjustments

Paleo-flood chronologies may help contextualize the geomorphic response of the Rio Moquegua. Using published (Magilligan and Goldstein 2001) and recently acquired radiocarbon dates (Table 3), we correlated terrace heights with basal floodplain and terrace ages (Figure 13). Using this correlation and the ASTER-derived DEM, we assigned estimated ages between measured valley fill heights (2-m contours) and radiocarbon age. This analysis indicates that 80 percent of the valley is younger than at least 550 ^{14}C yr BP (Figure 14). The oldest sampled date in the valley, 3250 ^{14}C yr BP, comes from a fan terrace complex near Tres Quebrada (Table 3). The top of the late Holocene fan terrace is $\sim$ 13 m above the modern channel bed, with only a few patches of higher surfaces existing in the valley. The young dates of alluvial material suggest that major channel migration has typified the past 550 yrs, with 80 percent of the 19.5 km study reach estimated to be younger than at least 550 radiocarbon years.

Discussion

Although climatically hyperarid, large floods have ravaged the Moquegua basin on both decadal and longer timescales with the potential to significantly affect physical and social conditions. Because of the broader climatic, geomorphic, and cultural implications of these

Table 3. Radiocarbon dates for terrace and floodplain surfaces

	Beta #	Site ID	Conventional ^{14}C yr BP	Intercept with calibration curve	Calibrated 1 sigma	Comments
Conde High Terrace	189086	CONDE-HT2003	550 ± 40	AD 1410	AD 1400–1420	Organic soil lens $\sim$ 1.46 m from terrace top
	180008	CONDE-HT-A	1130 ± 70	AD 900	AD 810–990	Organic soil lens $\sim$ 2.5 m below terrace top
Tres Quebrada Fan Terrace	180009	TQ-FAN-A-UP	3250 ± 70	1520 BC	1610–1440 BC	Peaty layer near fan base
Rio Moquegua Floodplain	180015	TQ-RB-TERR	560 ± 50	AD 1400	AD 1310–1420	Organic sediments in floodplain base
	189088	MOG-PAN-AM1	190 ± 60	AD 1670, 1780, 1800	AD 1650–1950	Organic sediments 67 cm below floodplain top
	189089	MOQ-PAN-AM2	60 ± 30	AD 1950	AD 1890–1950	Organic sediments 40 cm below floodplain top

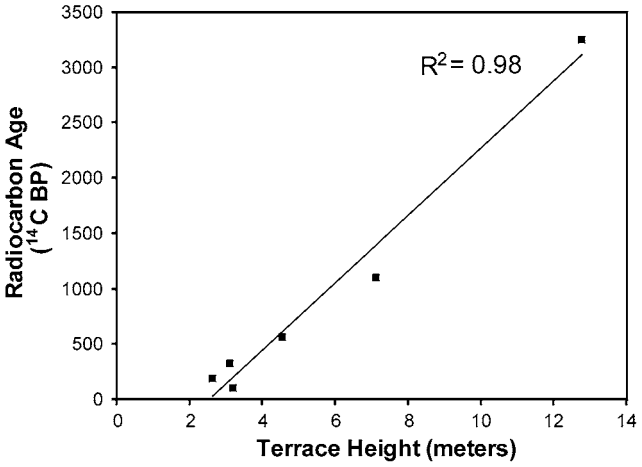

Figure 13. Correlation of terrace/floodplain heights with radiocarbon age. Terrace/floodplain heights are elevations above channel bed.

ENSO-related events, our documented flood history provides an important environmental and cultural context especially in linking the magnitude and pattern of floods to broader climatic and hydrologic regimes and the extension to regional cultural adjustments.

Climate and the Magnitude and Direction of Channel Change

Comparisons of flood timings to existing metrics of ENSOs fail to pinpoint channel activity with specific events although the La Niña in 1997 and El Niño in 1998 were previously field corroborated (Magilligan and Goldstein 2001), with the 1998 event having an estimated recurrence interval of $\sim$ 50–100 years. Certainly this event was not of the magnitude of the "mega-Niños" documented throughout Peru and the greater South Pacific (Wells 1990; Keefer et al. 1998; Nunn 2000; Magilligan and Goldstein 2001; Keefer, Moseley, and deFrance 2003), nevertheless it was associated with significant channel erosion in the Moquegua Valley especially following on the heels of the larger 1997 La Niña event. For the upper $\sim$ 10 km of the basin, this led to an average channel width increase of $\sim$ 25–30 m and significant floodplain scouring with an approximate loss of 6 percent of arable land.

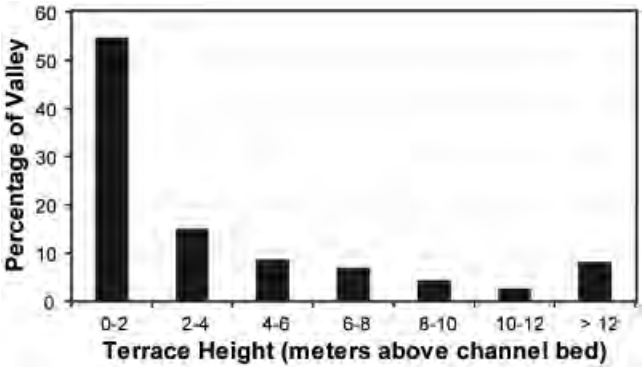

Figure 14. Histogram of elevations above channel bed for the total valley length (based on ASTER DEM) and percentage of valley within these 2-m contours. Histogram indicates that approximately 80 percent of the total valley is 6 m above the channel bed, where 6 m corresponds to $\sim$ 550 ^{14}C years BP from Figure 13.

Comparison with regional scale indices (Quinn, Neal, and Antunez de Mayolo 1987) did not often correspond specifically to channel-widening events. In some instances, extreme SOI values failed to materialize within the fluvial record, such as the 1982–1983 ENSO, but other times the associations were more apparent as in the 1997–1998 La Niña and El Niño sequence. The lack of correspondence may reflect the differences between marine/atmospheric measures of ENSO, such as the SOI, and the actual terrestrial expression of watershed scale precipitation and flooding. However, the comparison of decadal channel response and recovery based on aerial photography and GPS with the SOI (Figure 12) suggests that the magnitude and frequency of La Niña events may be as important, if not more important, in this region than the occurrence of El Niño events in explaining water availability and flood frequency.

Over the contemporary timescale afforded by aerial photography, average channel width ranges from approximately 78 to 120 m, and arable land within the currently irrigated floodplain ranges from 64 to 74 percent over the fifty-seven-year record. The rapid and extensive lateral migration following ENSO floods corresponds to the style of activity that occurs in other arid environments affected by ENSOs. Previous work in the southwest United States following the significant 1982–1983 ENSO indicates that most of the flood damage resulted from channel widening and lateral migration (Kresan 1988; Huckleberry 1994), which also seems to have occurred in the late Holocene (Huckleberry 1995, 1999; Waters and Ravesloot 2001, 2003). For the Moquegua Valley, where cut and fill periods may occur, the past several hundred years seem to have been dominated by lateral erosion. Extensive reworking of the valley seems to have begun at least 550 ^{14}C years ago (Figures 14) and tops of dated buried gravel bars ($\sim$ 1600 AD) correspond to the elevation of modern bar surfaces (Magilligan and Goldstein 2001), suggesting that valley incision has been limited over approximately the past 400 years.

Cultural Adaptation, Collapse, and the Tempo of Geomorphic Change

Archaeologists have long been interested in the relationship between climate change and cultural processes. In the Peruvian Andes, most of the attention has focused on droughts (Seltzer and Hastorf 1990; Shimada et al. 1991; Kolata and Ortloff 1996; Binford et al. 1997), yet large floods, especially those related to El Niño, may also result in acute social responses. Yet most of the interest in floods has been in extreme events that eradicate infrastructure like canals and other water delivery systems (Huckleberry 1999; Satterlee et al. 2000; Huckleberry and Billman 2003), or in the devastating effects on communities where debris flows spawned by ENSOs may instantaneously wipe out villages (Satterlee 1993; Keefer, Moseley, and deFrance 2003). Less attention has been given to the effects of floods on other landscape phenomena, specifically the loss and restoration of floodplain planting surfaces. For hypersensitive areas like the Moquegua Valley, where irrigated floodplain agriculture is the primary source of agricultural productivity, the links between geomorphology and culture may be profound. Our results on decadal scales indicate that floods with recurrence intervals of ~ 50 years may be associated with lateral erosion rates of ~ 2 ha/river km. In one of the few studies also linking channel lateral erosion with social response, Waters and Ravesloot (2001) documented a major period of channel widening ($\sim$ AD 1100) in the Gila River which led to Hohokam village abandonment and population rearrangements. In regions where the entire agricultural resource depends on irrigated floodplains, land may be as valuable as water, especially as populations approach regional carrying capacities (Dean 1988); in such regions the continued cannibalization of productive land by channel widening during floods may be an underappreciated mechanism for both terrestrial and social erosion (Ensor, Ensor, and DeVries 2003).

The tempo of geomorphic adjustments has an acute relationship with land use and therefore with social response (Hudson 2004). Channel widening during extreme events erodes productive land, requiring several decades to reconstitute to arable land. In these arid settings, vertical accretion rates are ~ 2–5 mm/yr (Magilligan and Goldstein 2001). If a period of continued channel erosion occurs, our results indicate that a minimum of 30 years may be required before the new alluvial material can be converted to productive land, assuming of course that no intervening catastrophic events occur. For some sustained periods, progressive and extensive lateral migration may dominate on submillennial timescales, and the channel may have sustained periods of floodplain stripping, with the result that young (and generally infertile) alluvium represents most of the valley fill.

The social responses to floodplain loss and recovery are difficult to elucidate but depend strongly on the magnitude and frequency of the hazard (Dean 1988; Waters and Ravesloot 2003). Societies have evolved intricate responses to mitigate the effect of hazards and have ritualized elaborate social mechanisms to lessen environmental hazards like droughts or floods. Social responses to rapid or sustained climate changes vary by the stochastic nature of the hazard and the ability of social systems to mitigate the effect. Our results suggest that floodplain loss following a succession of normal, high-frequency flood events may be a contributing factor to long-term social change, and is probably more significant than either catastrophic infrastructure loss or drought in riverine floodplain agricultural regimes. The approximately thirty-year timeframe for reconstituting arable land exceeds the generational timespan ($\sim 20+$ years) identified by Dean (1988) where social memory can deal effectively with high-frequency events. In societies like Moquegua's Formative Huaracane, with preexisting fracture lines of social stress like the growing tributary demands of elites, population increase, or competitive pressure from outside groups, the combination may have been fatal (Goldstein 2000b). We suspect that even incrementally increased episodes of floodplain erosion and decreased recovery rates could have been a significant factor in the decline of the Moquegua's floodplain-dependent Huaracane occupation of the valley in the mid–first millennium AD, and the competitive ascendancy of Tiwanaku colonists, who added diverse agricultural, political, and settlement strategies such as desert land reclamation, herding, and increased long distance exchange to the mix. Future research must determine to what degree the decline of the Huaracane (and, conversely, the competitive success of the Tiwanaku) is attributable to low-frequency events like the one documented for AD 700 (Magilligan and Goldstein 2001), or to a situation where tributary agricultural demands gradually outstripped the resilience of human response to the normal cycle of high frequency floods, land loss, and land regeneration.

Conclusions

Large floods have commonly occurred in this hyperarid environment of southern Peru, and the time series of response shown herein has documented the type, magnitude, and tempo of geomorphic change. On contem-

porary timescales, channel widening has been the dominant response to large floods with reach-averaged values of ~ 30 m occurring, which translates into an ~ 2 ha loss of arable floodplain per river kilometer. Irrigated floodplain agriculture is the dominant economic resource base, and the magnitude of lost land by erosion and the recovery rates have important social repercussions. For this hyperarid region of southern Peru, ENSO extremes dictate flood hydroclimatology and El Niños have been important flood-producing mechanisms on both contemporary and longer timescales and have been evoked as a causative factor in social collapse, as much as their part in severe and long-standing droughts in the highlands (Kolata and Ortloff 1996) and socially-devastating floods in coastal areas (Keefer, Moseley, and deFrance 2003).

Remote sensing and field analyses indicate that recovery is a two-stage process requiring in some cases upward of thirty years for arable land to be reconstituted, assuming the lack of an intervening large flood. Often, channel widening/narrowing corresponds to the decrease/increase of arable land, but channel narrowing may result more from lateral bar development that lacks immediate conversion to arable land. Probability transition matrices indicate that after a major channel-widening phase that occurred some time between 1946 and 1955, there was a sustained period of recovery, especially between 1976 and 1997; initial channel dimensions had been reattained by approximately 1970 but arable land peaks required an additional twenty-seven years to be achieved. The probability transition matrices are an effective technique to document the direction and rate of channel and riparian change.

On longer timescales, our results have several important extensions and ramifications. From a purely physical perspective, the contemporary pattern of response to extreme floods—lateral migration—appears to be the dominant channel behavior for the past ca. 500–600 years in this section of the Rio Moquegua. Combined radiocarbon dating and remote sensing surveys indicate that upwards of 80 percent of the valley is younger than at least 550 ^{14}C years. From a geoarchaeological perspective, the cannibalization of older alluvium further indicates that much of the mid-valley floodplain is culturally sterile (i.e., primarily post-contact) and that the pace of this lateral movement may have important implications for social and cultural conditions. Because the entire resource base depends on irrigated floodplain, land is as valuable as water in these environmentally stressed regions. If the tempo of landscape change by lateral migration outpaces reconstitution, severe physical stresses may result, perhaps resulting in social collapse as has been described for the Hohokam, and for the formative Huaracane and the Late Intermediate Chiribaya agriculturalists in Moquegua.

Within the broader framework of ENSOs, the timing and magnitude of geomorphic change seem conditioned by the magnitude of the Southern Oscillation Index, but exact relationships are difficult to establish. The Rio Moquegua lies in a sensitive region where Pacific-derived moisture sources, best described by low-phase SOI, may generate localized precipitation and subsequent large floods, as in 1998. Yet not all low-phase SOIs will affect these inland locations as is evident from the lack of a geomorphic signature of the 1982–1983 El Niño. More important is that the effects of La Niñas seem to materialize in the basin, and the pattern of channel widening and recovery accords well with the timing and magnitude of high phases of the SOI. As such, this research has shown the impact of ENSOs on both short-term and long-term geomorphic conditions and further research will hopefully reveal the longer-term history of ENSOs in this climatically sensitive and culturally rich region.

Acknowledgments

This research was funded in part by the Dartmouth College Rockefeller Center, the Dartmouth College Dickey Center for International Understanding, and the Dean of the Faculty Office at Dartmouth College. The authors would like to thank Mark Macklin, Hector Neff, and Dan Sandweiss for review comments that greatly improved the quality of the manuscript. Additional thanks go to the University of California Pacific Rim Research Program and the Museo Contisuyo, Moquegua. Jodie Davi and Heather Carlos helped with image analysis and cartography.

References

Baker, P. A., C. A. Rigsby, G. O. Seltzer, S. C. Fritz, T. K. Lowenstein, N. P. Bacher, and C. Veliz. 2001. Tropical climate changes at millennial and orbital timescales on the Bolivian Altiplano. *Nature* 409:698–701.

Baker, V. R. 1977. Stream-channel response to floods, with examples from central Texas. *Geological Society of America Bulletin* 88:1057–71.

Binford, M., A. Kolata, M. Brenner, J. Janusek, M. Seddon, M. Abbott, and J. Curtis. 1997. Climate variation and the rise and fall of an Andean civilization. *Quaternary Research* 47:235–48.

Caviedes, C. N. 2001. *El niño in history: Storming through the ages*. Gainesville: University Press of Florida.

Chapdelaine, C. 2000. Struggling for survival: The urban class of the Moche site, north coast of Peru. In *Environmental disaster and the archaeology of human response*, ed. G. Bawden and R. M. Reycraft, 121–42. Albuquerque: Maxwell Museum of Anthropology, University of New Mexico.

Chavez, F. P., J. Ryan, S. E. Lluch-Cota, and M. Niquen. 2003. From anchovies to sardines and back: Multi-decadal change in the Pacific Ocean. *Science* 299:217–21.

Clement, C. O., and M. E. Moseley. 1991. Spring-fed irrigation system of Carrizal, Peru: A case study of the hypothesis of agrarian collapse. *Journal of Field Archaeology* 18: 425–43.

Costa, J. E. 1974. Response and recovery of a Piedmont watershed from Tropical Storm Agnes, June 1972. *Water Resources Research* 10:106–12.

Dean, J. S. 1988. A model of Anasazi behavioral adaptation. In *The Anasazi in a changing environment*, ed. G. Gumerman, 25–44. Cambridge, U.K.: Cambridge University Press.

deMenocal, P. B. 2001. Cultural responses to climate change during the Late Holocene. *Science* 292 (5517): 667–73.

DeVries, T. J. 1987. A review of geological evidence for ancient El Niño activity in Peru. *Journal of Geophysical Research* 92:14471–79.

Ely, L. L., and P. K. House. 2000. Holocene flood activity in different regions of the western U.S. Annual GSA Meeting in Reno, Nevada. *Geological Society of America Abstracts with Programs* 32 (7): 512.

Ensor, B. E., M. O. Ensor, and G. W. DeVries. 2003. Hohokam political ecology and vulnerability: Comments on Waters and Ravesloot. *American Antiquity* 68:169–81.

Erickson, C. L. 1999. Neo-environmental determinism and agrarian "collapse" in Andean prehistory. *Antiquity* 73:634–42.

———. 2000. The Lake Titicaca Basin: A Precolumbian built landscape. In *Imperfect balance: Landscape transformations in the Precolumbian Americas*, ed. D. Lentz, 311–56. New York: Columbia University Press.

Fontugne, M., P. Usselmann, D. Lavallée, M. Julien, and C. Hatté. 1999. El Niño variability in the coastal desert of southern Peru during the mid-Holocene. *Quaternary Research* 52:171–79.

Formacion, S. P., and S. B. Saila. 1994. Markov chain properties related to temporal dominance changes in a Philippine pelagic fishery. *Fisheries Research* 19:241–56.

Goldstein, P. S. 1989. Omo, a Tiwanaku provincial center in Moquegua Peru. PhD diss., University of Chicago.

———. 1993. Tiwanaku temples and state expansion: A Tiwanaku sunken court temple in Moquegua, Peru. *Latin American Antiquity* 4:22–47.

———. 2000a. Communities without borders: The vertical archipelago, and diaspora communities in the southern Andes. In *The archaeology of communities: A New World perspective*, ed. J. Yaeger and M. Canuto, 182–209. New York: Routledge.

———. 2000b. Exotic goods and everyday chiefs: Long distance exchange and indigenous sociopolitical development in the south central Andes. *Latin American Antiquity* 11 (4): 1–27.

———. 2003. From stew-eaters to maize-drinkers: The Chicha economy and Tiwanaku. In *Pots as political tools: The culinary equipment of early imperial states in comparative perspective*, ed. T. Bray, 143–72. New York: Kluwer Academic.

———. 2005. *Andean diaspora: The Tiwanaku colonies and the origins of Andean empire*. Gainesville: University Press of Florida.

Gregory-Wodzicki, K. M. 2000. Uplift history of the central and northern Andes: A review. *Geological Society America Bulletin* 112:1091–1105.

Grosjean, M., L. Nunez, I. Cartajena, and B. Messerli. 1997. Mid-Holocene climate and culture change in the Atacama Desert, northern Chile. *Quaternary Research* 48:239–46.

Houston, J. 2002. Groundwater recharge through an alluvial fan in the Atacama Desert, northern Chile: Mechanisms, magnitudes and causes. *Hydrological Processes* 16 (15): 3019–35.

Houston, J., and A. J. Hartley. 2003. The central Andean west-slope rainshadow and its potential contribution to the origin of hyper-aridity in the Atacama Desert. *International Journal of Climatology* 23 (12): 1453–64.

Huckleberry, G. A. 1994. Contrasting channel response to floods on the middle Gila River, Arizona. *Geology* 22:1083–86.

———. 1995. Archaeological implications of late Holocene channel changes on the middle Gila River, Arizona. *Geoarchaeology—An International Journal* 10:159–82.

———. 1999. Stratigraphic identification of destructive floods in relict canals: A case study from the middle Gila River, Arizona. *Kiva* 86:7–33.

Huckleberry, G. A., and B. R. Billman. 2003. Geoarchaeological insights gained from surficial geologic mapping, middle Moche Valley, Peru. *Geoarchaeology—An International Journal* 18:505–21.

Hudson, P. F. 2004. Geomorphic context of the prehistoric Huastec floodplain environments: Lower Panuco basin, Mexico. *Journal of Archaeological Science* 31:653–68.

Keefer, D. K., S. D. deFrance, M. E. Moseley, J. B. Richardson, D. R. Satterlee, and A. Day-Lewis. 1998. Early maritime economy and El Niño events at Quebrada Tacahuay, Peru. *Science* 281:1833–35.

Keefer, D. K., M. E. Moseley, and S. D. deFrance. 2003. A 38000-year record of floods and debris flows in the Ilo region of southern Peru and its relation to El Niño events and great earthquakes. *Palaeogeography Palaeoclimatology Palaeoecology* 194 (1–3): 41–77.

Kerr, R. A. 1999. El Niño grew strong as cultures were born. *Science* 283:467–68.

Kolata, A. L. 2000. Environmental thresholds and the "natural history" of an Andean civilization. In *Environmental disaster and the archaeology of human response*, ed. G. Bawden and R. Martin, 163–78. Albuquerque: Maxwell Museum of Anthropology, University of New Mexico.

Kolata, A. L., M. W. Binford, M. Brenner, J. W. Janusek, and C. Ortloff. 2000. Environmental thresholds and the empirical reality of state collapse: A response to Erickson (1999). *Antiquity* 74:424–26.

Kolata, A. L., and C. R. Ortloff. 1996. Agroecological perspectives on the decline of the Tiwanaku state. In *Tiwanaku and its hinterland: Archaeology and paleoecology of an Andean civilization*, ed. A. L. Kolata, 181–202. Washington, DC: Smithsonian Institution Press.

Kresan, P. L. 1988. The Tucson, Arizona flood of October 1983: Implications for land management along alluvial river channels. In *Flood geomorphology*, ed. V. Baker, R. C. Kochel, and P. C. Patton, 465–89. New York: Wiley.

Maas, G., and M. G. Macklin. 2002. The impact of recent climate change on flooding and sediment supply within a Mediterranean mountain catchment, southwestern Crete, Greece. *Earth Surface Processes and Landforms* 27: 1087–1105.

Maas, G. S., M. G. Macklin, J. Warburton, J. C. Woodward, and E. Meldrum. 2001. A 300 year history of flooding in an Andean mountain river system: The river Alizos, southern Bolivia. In *River basin sediment systems*, ed. D. A. Maddy, M. G. Macklin, and J. C. Woodward, 297–323. Rotterdam: A.A. Balkema.

Magilligan, F. J., and P. S. Goldstein. 2001. El Niño floods and culture change: A late Holocene flood history for the Rio Moquegua, southern Peru. *Geology* 29:431–34.

Magilligan, F. J., J. D. Phillips, B. Gomez, and L. A. James. 1998. Geomorphic and sedimentological controls on the effectiveness of an extreme flood. *Journal of Geology* 106:87–95.

Magilligan, F. J., and M. L. Stamp. 1997. Historical land-cover changes and hydrogeomorphic adjustment in a small Georgia watershed. *Annals Association of American Geographers* 87:614–35.

McPhaden, M. J. 1999. Genesis and evolution of the 1997–1998 El Niño. *Science* 283:950–54.

Miller, A. J. 1995. Valley morphology and boundary conditions influencing spatial patterns of flood flow. In *Natural and anthropogenic influences in fluvial geomorphology*, ed. J. Costa, A. Miller, K. Potter, and P. Wilcock, 57–82. Washington, DC: AGU.

Moseley, M. E. 1997. Climate, culture and punctuated change: New data, new challenges. *The Review of Archaeology* 18:19–27.

———. 2000. Confronting natural disaster. In *Environmental disaster and the archaeology of human response*, ed. G. Bawden and R. M. Reycraft, 219–23. Albuquerque: Maxwell Museum of Anthropology, University of New Mexico.

Moseley, M. E., R. A. Feldman, C. R. Ortloff, and A. Narvaez. 1983. Principles of agrarian collapse in the Cordillera Negra, Peru. *Annals of Carnegie Museum* 52:299–327.

Moseley, M. E., and J. B. Richardson. 1992. Doomed by natural disaster. *Archaeology* 45:44–5.

Moseley, M. E., D. Warner, and J. B. Richardson. 1992. Space shuttle imagery of recent catastrophic change along the arid Andean coast. In *Paleoshorelines and prehistory: An exploration of method*, ed. L. L. Johnson and M. Straight, 215–35. Boca Raton: CRC Press.

Nunn, P. D. 2000. Environmental catastrophe in the Pacific Islands around A.D. 1300. *Geoarchaeology* 15 (7): 715–40.

Ortlieb, L. 2000. The documented historical record of El Niño events in Peru: An update of the Quinn Record (sixteenth through nineteenth centuries). In *El Niño and the Southern Oscillation: Multiscale variability and global and regional impacts*, ed. H. F. Diaz and V. Markgraf, 207–97. Cambridge, U.K.: Cambridge University Press.

Ortlieb, L., M. Fournier, and J. Macharé. 1993. Beach-ridge series in northern Peru: Chronology, correlation and relationship with major Late Holocene El Niño events. *Bulletin de l'Institut Français d'Etudes Andines* 22:191–212.

Ortlieb, L., and J. Machare. 1993. Former El-Niño events: Records from western South America. *Global and Planetary Change* 7:181–202.

Pitlick, J. 1993. Response and recovery of a subalpine stream following a catastrophic flood. *Geological Society of American Bulletin* 105:657–70.

Placzek, C., J. Quade, and J. L. Betancourt. 2001. Holocene lake level fluctuations of Lago Aricota, southern Peru. *Quaternary Research* 56:181–90.

Poole, G., J. Stanford, C. Frissell, and S. Running. 2002. Three-dimensional mapping of geomorphic controls on flood-plain hydrology and connectivity from aerial photos. *Geomorphology* 48:329–47.

Quinn, W., V. Neal, and S. E. Antunez de Mayolo. 1987. El Niño occurrences over the past four and a half centuries. *Journal of Geophysical Research* 92:14449–61.

Reycraft, R. M. 2000. Long-term human response to El Niño in south coastal Peru, circa A.D. 1400. In *Environmental disaster and the archaeology of human response*, ed. G. Bawden and R. M. Reycraft, 99–119. Albuquerque: Maxwell Museum of Anthropology, University of New Mexico.

Richardson, J. B. 1983. The Chira beach ridges, sea level change, and the origins of maritime economies on the Peruvian coast. *Annals of Carnegie Museum* 52:265–75.

Rinaldi, M. 2003. Recent channel adjustments in alluvial rivers of Tuscany, central Italy. *Earth Surface Processes and Landforms* 28:587–608.

Ritter, D. F., R. G. Kochel, and J. R. Miller. 1999. The disruption of Grassy Creek: Implications concerning catastrophic events and thresholds. *Geomorphology* 29:323–38.

Rogers, S. S., D. H. Sandweiss, K. A. Maasch, D. F. Belknap, and P. Agouris. 2004. Coastal change and beach ridges along the northwest coast of Peru: Image and GIS analysis of the Chira, Piura, and Colan beach-ridge plains. *Journal of Coastal Research* 20 (4): 1102–25.

Rumsby, B. T., and M. G. Macklin. 1994. Channel and floodplain response to recent abrupt climate-change: The Tyne Basin, Northern England. *Earth Surface Processes and Landforms* 19 (6): 499–515.

Sandweiss, D. H. 1986. The beach ridges at Santa, Peru: El Niño, uplift and prehistory. *Geoarchaeology* 1:17–28.

Sandweiss, D. H., K. A. Maasch, D. F. Belknap, J. B. Richardson, and H. B. Rollins. 1998. Discussion of: Lisa E. Wells, 1996. The Santa Beach Ridge complex (which appeared in *Journal of Coastal Research* 12:1–17). *Journal of Coastal Research* 14 (1): 367–73.

Sandweiss, D. H., K. A. Maasch, R. L. Burger, J. B. Richardson, H. B. Rollins, and A. Clement. 2001. Variation in Holocene El Niño frequencies: Climate records and cultural consequences in ancient Peru. *Geology* 29:603–06.

Satterlee, D. R. 1993. *The impact of a fourteenth century El Niño flood on an indigenous population near Ilo, Peru*. PhD diss., University of Florida.

Satterlee, D. R., M. E. Moseley, D. M. Keefer, and J. E. A. Tapia. 2000. The Miraflores El Niño disaster: Convergent catastrophes and prehistoric agrarian change in southern Peru. *Andean Past* 6:95–116.

Schumm, S. A., and R. W. Lichty. 1963. Channel widening and flood-plain construction along Cimarron River in southwestern Kansas. USGS Professional Paper 352-D, pp. 71–88.

Selim, S. Z., and A. H. Al-Rabeh. 1995. Determining dominant wind directions. *European Journal of Operational Research* 90:420–26.

Seltzer, G. O., and C. A. Hastorf. 1990. Climatic change and its effect on Prehispanic agriculture in the central Peruvian Andes. *Journal of Field Archaeology* 17:397–414.

Shimada, I., C. B. Schaaf, L. Thompson, and E. Moseley-Thompson. 1991. Cultural impacts of severe droughts in

the Prehistoric Andes: Application of a 1,500-year ice core precipitation record. *World Archaeology* 22:247–70.

Sloan, J., J. R. Miller, and N. Lancaster. 2001. Response and recovery of the Eel River, California and its tributaries to floods in 1955, 1964 and 1997. *Geomorphology* 36:129–54.

Thouret, J.-C., J. Davila, and J.-P. Eisen. 1999. Largest explosive eruption in historical times in the Andes at Huaynaputina volcano, A.D. 1600, southern Peru. *Geology* 27:435–38.

Tosdal, R. M., A. H. Clark, and E. Farrar. 1984. Cenozoic polyphase landscape and tectonic evolution of the Cordillera Occidental, southernmost Peru. *Geological Society of America Bulletin* 95:1318–32.

Vuille, M. 1999. Atmospheric circulation over the Bolivian Altiplano during dry and wet periods and extreme phases of the Southern Oscillation. *International Journal of Climatology* 19:1579–1600.

Waters, M. R., and J. C. Ravesloot. 2001. Landscape change and the cultural evolution of the Hohokam along the middle Gila River and other river valleys in south-central Arizona. *American Antiquity* 66:285–99.

———. 2003. Disaster or catastrophe: Human adaptation to high- and low- frequency landscape processes; A reply to Ensor, Ensor, and DeVries. *American Antiquity* 68:400–5.

Weiss, H. 2000. Beyond the Younger Dryas. In *Environmental disaster and the archaeology of human response*, ed. G. Bawden and R. M. Reycraft, 75–98. Albuquerque: Maxwell Museum of Anthropology, University of New Mexico.

Weiss, H., M.-A. Courty, W. Wetterstrom, F. Guichard, L. Senior, R. Meadow, and A. Curnow. 1993. The genesis and collapse of Third Millennium North Mesopotamian civilization. *Science* 261:995–1004.

Wells, L. E. 1990. Holocene history of the El Niño phenomenon as recorded in flood sediments on northern coastal Peru. *Geology* 18:1134–37.

———. 1996. The Santa beach ridge complex: Sea level and progradational history of an open gravel coast in central Peru. *Journal of Coastal Research* 12:1–17.

Wells, L. E., and J. S. Noller. 1999. Holocene coevolution of the physical landscape and human settlement in northern coastal Peru. *Geoarchaeology* 14:755–89.

Williams, R. P. 1997. Disaster in the development of agriculture and the evolution of social complexity in the south-central Andes. PhD diss., University of Florida.

———. 2002. Rethinking disaster-induced collapse in the demise of the Andean highland states: Wari and Tiwanaku. *World Archaeology* 33:361–74.

Winterbottom, S. 2000. Medium and short-term channel planform changes on the Rivers Tay and Tummel, Scotland. *Geomorphology* 34:195–208.

Wolman, M. G., and R. Gerson. 1978. Relative scales of time and effectiveness of climate in watershed geomorphology. *Earth Surface Processes* 3:189–208.

Wolman, M. G., and J. P. Miller. 1960. Magnitude and frequency of forces in geomorphic processes. *Journal of Geology* 68: 54–74.

Wolter, K., and M. S. Timlin. 1998. Measuring the strength of ENSO events: How does the 1997/8 rank? *Weather* 53:315–24.

Yu, P. S., and T. C. Yang. 1997. A probability-based renewal rainfall model for flow forecasting. *Natural Hazards* 15:51–70.

Correspondence: Department of Geography, University of North Carolina, Chapel Hill, NC 27599-3220, e-mail: manners@interfluve.com (Manners); Department of Geography, Dartmouth College, Hanover, NH 03755, e-mail: francis.j.magilligan@dartmouth.edu (Magilligan; corresponding author); Department of Anthropology, UC San Diego, La Jolla, CA 92093-0532, e-mail: psgoldst@weber.ucsd.edu (Goldstein).